Progress In Electromagnetics Research B, Vol. 33, 175–202, 2011

A NEGATIVE REFRACTIVE INDEX METAMATERIAL BASED ON A CUBIC ARRAY OF LAYERED NONMAGNETIC SPHERICAL PARTICLES

E. F. Kuester[1,*], N. Memić[1], S. Shen[1], A. Scher[1], S. Kim[1], K. Kumley[1], and H. Loui[2]

[1]Department of Electrical, Computer and Energy Engineering, University of Colorado, 425 UCB, Boulder, CO 80309-0425, USA

[2]SAR Sensor Technologies, Sandia National Laboratories, Albuquerque, NM 87185-0529, USA

Abstract—A low-loss passive metamaterial exhibiting negative refractive index or "double negative" electromagnetic properties at microwave frequencies is proposed. The metamaterial is a lattice of spherical particles made up of multiple dielectric materials in concentric layers. Because no magnetic constituents (that tend to have higher losses) are involved, the negative-index behavior is possible with very low values of attenuation. A negative-index metamaterial based on dielectric-coated metal spheres is also proposed, and is predicted to have lower attenuation than other structures based on metallic scatterers. Numerical results and design principles are given.

1. INTRODUCTION

Metamaterials possessing negative dielectric permittivity and/or magnetic permeability have been actively investigated in recent years. The first metamaterial shown to exhibit negative refractive index or "double negative" (DNG) behavior was an array of conducting split-ring resonators and rods arranged in a lattice [1]. This class of materials has several drawbacks for many applications: losses are often unacceptably high, and the material has a natural anisotropy which must be overcome by re-orienting the elements of the array in different directions. Recently, an alternative DNG metamaterial was proposed that is naturally isotropic — a cubic lattice of magnetodielectric

Received 22 April 2011, Accepted 20 July 2011, Scheduled 30 July 2011

* Corresponding author: Edward F. Kuester (kuester@colorado.edu).

spherical particles, whose Lorenz-Mie resonances induce an effective permittivity and permeability that can be set to any desired values by choosing the lattice and particle parameters appropriately [2]. It was hoped that this approach would also lead to reduced losses in the metamaterial, but since the particles need to have large permeability as well as large permittivity, the associated losses near resonance are generally still too large to address this drawback.

Several researchers have proposed variants of the idea presented in [2] that avoid the use of materials having magnetic permeabilities different from vacuum. In [3–13], it is proposed that two different sizes of purely dielectric spheres be alternated in the lattice, chosen so that the dielectric resonance frequency of one sphere size is adjusted to coincide with the magnetic resonance frequency of the other sphere size. This has the advantage of employing only dielectric materials, which are often inherently of very low loss, but suffers from additional structural complexity, complicating the fabrication process. In [14], a similar idea is proposed, but in which one set of spheres are of ordinary dielectric material and contribute to a negative permeability, while the other set is composed of a plasma semiconductor, which contributes a negative permittivity. A variation on this idea was proposed in [15], wherein only one set of purely dielectric spheres is used (to generate negative permeability), but embedded in a negative permittivity host (such as semiconductor plasma). Wheeler et al. [16] (and later Yannopapas [17]) have proposed a lattice of two-layered spheres, in which one layer is ordinary dielectric and the other a semiconducting plasma, in order to realize a negative-index medium. Khoo et al. [18] have extended this idea by using a liquid crystal as the host medium in order to achieve tunability of the effective properties. The presence of plasma constituents in these designs will lead to increased losses by comparison with realizations using only low-loss dielectrics. Finally, a sort of "meta-metamaterial" is proposed in [19], in which layered spheres, themselves made up of metamaterials having negative permittivity and/or permeability, are arranged in a lattice to achieve the desired overall effective material properties. While offering potentially very great design flexibility, this approach will also present formidable fabrication and size problems in practice.

In this paper, we propose a new approach that yields a passive metamaterial that exhibits far lower losses at microwave frequencies than anything that has heretofore appeared in the literature. The structure is a cubic periodic array of layered dielectric spheres, made from low-loss high-permittivity ceramics. Although the geometry is the same as that of [16–18], our structure does not use metals or semiconductors, thereby achieving much less attenuation than those

designs. We begin by reviewing the effective medium properties of an array of homogeneous magnetodielectric spheres, and then present a critical review of the formulas for two-layered spheres, correcting in the process a number of errors that have been published in previous literature. We then present numerical results of a "brute-force" search for combinations of parameters that result in a negative effective refractive index for the proposed metamaterial. Some discussion of the parameter ranges required to achieve this is carried out, and comparison with finite-element simulations is made to validate our analysis. Finally, another negative-index metamaterial is proposed that is based on dielectric-coated metallic spheres. Although lossier than the all-dielectric metamaterial, this structure still offers lower attenuation than has been achieved by those proposed up to now.

2. EFFECTIVE MEDIUM EQUATIONS

2.1. Array of Homogeneous Spheres — Review

The tools for expressing the effective permittivity and permeability of a composite medium consisting of a lattice of resonant spheres have existed for a surprisingly long time. In fact, one year after the publication of Mie's paper [20] on the scattering of electromagnetic waves by a uniform magnetodielectric sphere[†], Gans and Happel [23] derived expressions for the effective material parameters of a cubic lattice of such spheres, using the dipole scattering coefficients from Mie's solution (see also [24] and [25]). We follow this procedure here.

The geometry involved is shown in Fig. 1. Homogeneous spheres of permittivity ϵ_2, permeability μ_2 and radius a are arranged in a cubic lattice of period (lattice constant) p in a background medium whose electromagnetic parameters are ϵ_1 and μ_1. A time dependence of $e^{j\omega t}$ will be assumed, and we will define the wavenumbers $k_1 = \omega\sqrt{\mu_1\epsilon_1}$ and $k_2 = \omega\sqrt{\mu_2\epsilon_2}$ in the background and sphere media respectively.

The classical Clausius-Mossotti-Lorentz-Lorenz formulas express the effective permittivity and permeability of such a medium in terms of the electric and magnetic polarizabilities α_e and α_m of the "atoms" of the composite medium (here, the spheres):

$$\epsilon_{\text{eff}} = \epsilon_1 \frac{1 + 2N\alpha_e}{1 - N\alpha_e} \tag{1}$$

$$\mu_{\text{eff}} = \mu_1 \frac{1 + 2N\alpha_m}{1 - N\alpha_m} \tag{2}$$

[†] Although this scattering problem is often referred to only by Mie's name, many others, most notably Lorenz, have made equally significant contributions. See [21, Section 3.4] and [22] for an extensive historical assessment.

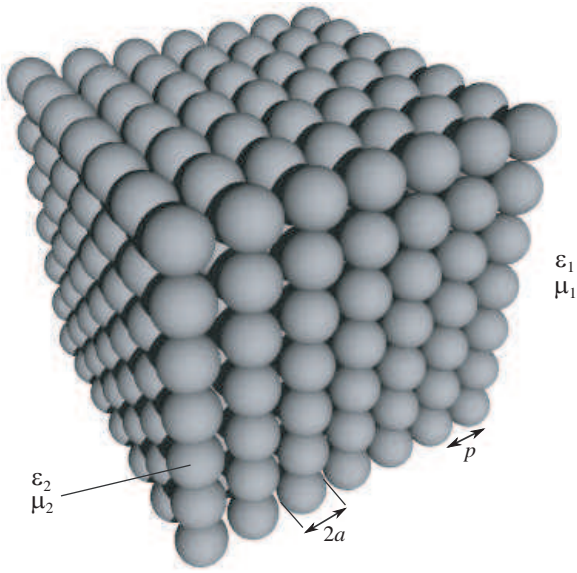

Figure 1. Cubic array of homogeneous magnetodielectric spheres.

where $N = p^{-3}$ is the volume density of the spheres. The polarizabilities for a homogeneous sphere can be expressed for nonzero frequency in terms of the dipole-order Lorenz-Mie coefficients of the resonant spheres (see, e.g., [26, Eq. (4.53)], where the result for differing magnetic properties is given):

$$\alpha_e = -\frac{2\pi j a_1}{k_1^3} \tag{3}$$

$$\alpha_m = -\frac{2\pi j b_1}{k_1^3} \tag{4}$$

where

$$a_1 = \frac{\sqrt{\epsilon_r}\psi_1'(k_1a)\psi_1(k_2a) - \sqrt{\mu_r}\psi_1(k_1a)\psi_1'(k_2a)}{\sqrt{\epsilon_r}\xi_1'(k_1a)\psi_1(k_2a) - \sqrt{\mu_r}\xi_1(k_1a)\psi_1'(k_2a)} \tag{5}$$

$$b_1 = \frac{\sqrt{\mu_r}\psi_1'(k_1a)\psi_1(k_2a) - \sqrt{\epsilon_r}\psi_1(k_1a)\psi_1'(k_2a)}{\sqrt{\mu_r}\xi_1'(k_1a)\psi_1(k_2a) - \sqrt{\epsilon_r}\xi_1(k_1a)\psi_1'(k_2a)} \tag{6}$$

Here $\epsilon_r = \epsilon_2/\epsilon_1$ and $\mu_r = \mu_2/\mu_1$ are the values of the sphere parameters relative to those of the background, and $\psi_1(z)$ and $\xi_1(z) = \psi_1(z) + j\chi_1(z)$ are Riccati-Bessel functions, expressed by means of

standard spherical Bessel functions[‡] in terms of elementary functions:

$$\psi_1(z) = zj_1(z) = \frac{\sin z - z\cos z}{z} \tag{7}$$

$$\chi_1(z) = -zy_1(z) = \frac{\cos z + z\sin z}{z} \tag{8}$$

Thus, the effective parameters of the composite medium are given by:

$$\epsilon_{\text{eff}} = \epsilon_1 \frac{1 - 4\pi jNa_1/k_1^3}{1 + 2\pi jNa_1/k_1^3} \tag{9}$$

$$\mu_{\text{eff}} = \mu_1 \frac{1 - 4\pi jNb_1/k_1^3}{1 + 2\pi jNb_1/k_1^3} \tag{10}$$

If the results of Gans and Happel [23, Eqs. (46)–(47)] are written in the notation used here, and higher-order non-dipolar terms omitted from their expression for ϵ_{eff}, they are found to be identical to (9)–(10). Equivalent results for the case where $\mu_1 = \mu_2 = \mu_0$ were also obtained recently by Wheeler et al. [16, Eqs. (1), (2), (7) and (8)].

The applicability of an effective medium description requires the lattice constant p to be sufficiently small compared to a wavelength in the background medium [2, 28]. Thus, it really only makes sense to use (9)–(10) or (1)–(2) in the limit $k_1 a \ll 1$ (but not necessarily $k_2 a \ll 1$). In this case, the Riccati-Bessel functions of $k_1 a$ can be replaced by their small-argument approximations:

$$\psi_1(z) \simeq \frac{z^2}{3}; \quad \psi_1'(z) \simeq \frac{2z}{3}; \quad \chi_1(z) \simeq \frac{1}{z}; \quad \chi_1'(z) \simeq -\frac{1}{z^2} \tag{11}$$

resulting in

$$a_1 = \frac{2j}{3}(k_1 a)^3 \frac{\epsilon_r F(k_2 a) - 1}{\epsilon_r F(k_2 a) + 2} \tag{12}$$

$$b_1 = \frac{2j}{3}(k_1 a)^3 \frac{\mu_r F(k_2 a) - 1}{\mu_r F(k_2 a) + 2} \tag{13}$$

where we have defined the function [28]

$$F(z) = \frac{2\psi_1(z)}{z\psi_1'(z)} = \frac{2(\sin z - z\cos z)}{z\cos z + (z^2 - 1)\sin z} \tag{14}$$

Note that in numerical calculations, it may be preferable to use one of the approximate forms

$$F(z) \simeq \frac{2(1 - jz)}{z^2 - 1 + jz}; \quad \text{if } \text{Im}(z) < -10 \tag{15}$$

[‡] The notation for spherical Bessel functions j_ν and y_ν is that used in Abramowitz and Stegun [27]. The notation for Riccati-Bessel functions is not standardized, and we have used that of [21].

or

$$F(z) \simeq \frac{10 - z^2}{10 - 2z^2}; \quad \text{if } |z| \ll 1 \tag{16}$$

for $F(z)$. Inserting (12)–(13) into (9)–(10) gives

$$\epsilon_{\text{eff}} = \epsilon_1 \frac{1 + 2f\frac{\epsilon_r F(k_2 a) - 1}{\epsilon_r F(k_2 a) + 2}}{1 - f\frac{\epsilon_r F(k_2 a) - 1}{\epsilon_r F(k_2 a) + 2}} \tag{17}$$

$$\mu_{\text{eff}} = \mu_1 \frac{1 + 2f\frac{\mu_r F(k_2 a) - 1}{\mu_r F(k_2 a) + 2}}{1 - f\frac{\mu_r F(k_2 a) - 1}{\mu_r F(k_2 a) + 2}} \tag{18}$$

where

$$f = \frac{4\pi a^3 N}{3} = \frac{4\pi a^3}{3p^3} \tag{19}$$

is the volume fraction occupied by the spheres. Eqs. (17) and (18) were given by Lewin [28], and obtained in a more general context by Khizhnyak [29] (see also the references cited in [2]).

2.2. Array of Two-layered Spheres — Critical Analysis

This same approach can be used for a composite medium made up of layered spheres, if the appropriate generalization of Mie's analysis is used (see the original papers [30–32] as well as the treatments in the books [21, Sections 5.1-5.2] and [26, Section 8.1]). We limit our treatment to spheres with only two layers, as shown in Fig. 2. The outer radius of the particle is still a, and the outer layer still has material properties ϵ_2 and μ_2, but this medium surrounds a core of radius b and material parameters ϵ_3, μ_3.

Of the references cited above, only [30] gives expressions for the modified Lorenz-Mie coefficients of a two-layer sphere when there is contrast in the magnetic properties as well as the dielectric ones (these results can be found quoted elsewhere, in [33] and [34] for example). Their results can be written in our notation as:[§]

$$a_1 = \frac{\sqrt{\epsilon_{r21}}\psi_1'(k_1 a)G_\epsilon(k_2 a) - \sqrt{\mu_{r21}}\psi_1(k_1 a)G_\epsilon'(k_2 a)}{\sqrt{\epsilon_{r21}}\xi_1'(k_1 a)G_\epsilon(k_2 a) - \sqrt{\mu_{r21}}\xi_1(k_1 a)G_\epsilon'(k_2 a)} \tag{20}$$

[§] Aden and Kerker [30] use a notation for the Riccati-Bessel functions that can be confused with what is now the standard for spherical Bessel functions, and Alù and Engheta [19] have followed their choice. Kerker [21, p. 194] gives a table to help clarify the notations used in various treatments.

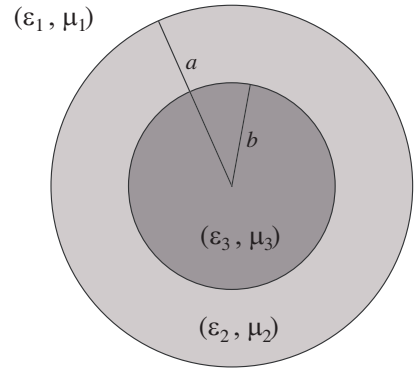

Figure 2. A two-layered sphere.

where

$$A_1 = \frac{\sqrt{\epsilon_{r32}}\psi_1'(k_2b)\psi_1(k_3b) - \sqrt{\mu_{r32}}\psi_1(k_2b)\psi_1'(k_3b)}{\sqrt{\epsilon_{r32}}\chi_1'(k_2b)\psi_1(k_3b) - \sqrt{\mu_{r32}}\chi_1(k_2b)\psi_1'(k_3b)}$$
$$= \frac{\epsilon_{r32}F(k_3b)\frac{k_2b}{2}\psi_1'(k_2b) - \psi_1(k_2b)}{\epsilon_{r32}F(k_3b)\frac{k_2b}{2}\chi_1'(k_2b) - \chi_1(k_2b)} \tag{21}$$

and

$$G_\epsilon(z) = \psi_1(z) - A_1\chi_1(z) \tag{22}$$

while

$$b_1 = \frac{\sqrt{\mu_{r21}}\psi_1'(k_1a)G_\mu(k_2a) - \sqrt{\epsilon_{r21}}\psi_1(k_1a)G_\mu'(k_2a)}{\sqrt{\mu_{r21}}\xi_1'(k_1a)G_\mu(k_2a) - \sqrt{\epsilon_{r21}}\xi_1(k_1a)G_\mu'(k_2a)} \tag{23}$$

where

$$B_1 = \frac{\sqrt{\mu_{r32}}\psi_1'(k_2b)\psi_1(k_3b) - \sqrt{\epsilon_{r32}}\psi_1(k_2b)\psi_1'(k_3b)}{\sqrt{\mu_{r32}}\chi_1'(k_2b)\psi_1(k_3b) - \sqrt{\epsilon_{r32}}\chi_1(k_2b)\psi_1'(k_3b)}$$
$$= \frac{\mu_{r32}F(k_3b)\frac{k_2b}{2}\psi_1'(k_2b) - \psi_1(k_2b)}{\mu_{r32}F(k_3b)\frac{k_2b}{2}\chi_1'(k_2b) - \chi_1(k_2b)} \tag{24}$$

and

$$G_\mu(z) = \psi_1(z) - B_1\chi_1(z) \tag{25}$$

Here, $\epsilon_{r21} = \epsilon_2/\epsilon_1$, $\epsilon_{r32} = \epsilon_3/\epsilon_2$, $\mu_{r21} = \mu_2/\mu_1$ and $\mu_{r32} = \mu_3/\mu_2$ are ratios of the material properties in adjacent layers. If $\mu_1 = \mu_2 = \mu_3 = \mu_0$ and $\epsilon_1 = \epsilon_0$, we recover the results of [16, Eqs. (18)–(21)]. It is readily checked that these expressions reduce to the appropriate limits (5) and (6) for a homogeneous sphere if we take $b = 0$, $b = a$, or $\epsilon_3 = \epsilon_2$ and $\mu_3 = \mu_2$.

If we take $k_1 a \ll 1$ as we did for the homogeneous sphere and use (11), Eqs. (20) and (23) become

$$a_1 = \frac{2j}{3}(k_1 a)^3 \frac{\epsilon_{r21} F_2(k_2 a, A_1) - 1}{\epsilon_{r21} F_2(k_2 a, A_1) + 2} \tag{26}$$

$$b_1 = \frac{2j}{3}(k_1 a)^3 \frac{\mu_{r21} F_2(k_2 a, B_1) - 1}{\mu_{r21} F_2(k_2 a, B_1) + 2} \tag{27}$$

where

$$F_2(z, q) = \frac{2[\psi_1(z) - q\chi_1(z)]}{z[\psi_1'(z) - q\chi_1'(z)]} \tag{28}$$

Introducing three types of cross-products of the Riccati-Bessel functions and their derivatives, some of whose properties are catalogued in Appendix A,

$$C_1(z_1, z_2) = \psi_1(z_1)\chi_1(z_2) - \chi_1(z_1)\psi_1(z_2) \tag{29}$$

$$C_2(z_1, z_2) = \psi_1(z_1)\chi_1'(z_2) - \chi_1(z_1)\psi_1'(z_2) \tag{30}$$

$$C_3(z_1, z_2) = \psi_1'(z_1)\chi_1'(z_2) - \chi_1'(z_1)\psi_1'(z_2) \tag{31}$$

we can write, after some algebra,

$$F_2(k_2 a, A_1) = \frac{2}{k_2 a} \frac{\epsilon_{r32} \frac{k_2 b}{2} F(k_3 b) C_2(k_2 a, k_2 b) - C_1(k_2 a, k_2 b)}{\epsilon_{r32} \frac{k_2 b}{2} F(k_3 b) C_3(k_2 a, k_2 b) + C_2(k_2 b, k_2 a)} \tag{32}$$

$$F_2(k_2 a, B_1) = \frac{2}{k_2 a} \frac{\mu_{r32} \frac{k_2 b}{2} F(k_3 b) C_2(k_2 a, k_2 b) - C_1(k_2 a, k_2 b)}{\mu_{r32} \frac{k_2 b}{2} F(k_3 b) C_3(k_2 a, k_2 b) + C_2(k_2 b, k_2 a)} \tag{33}$$

Inserting (26)–(27) into (9)–(10) gives

$$\epsilon_{\text{eff}} = \epsilon_1 \frac{1 + 2f \frac{\epsilon_{r21} F_2(k_2 a, A_1) - 1}{\epsilon_{r21} F_2(k_2 a, A_1) + 2}}{1 - f \frac{\epsilon_{r21} F_2(k_2 a, A_1) - 1}{\epsilon_{r21} F_2(k_2 a, A_1) + 2}} \tag{34}$$

$$\mu_{\text{eff}} = \mu_1 \frac{1 + 2f \frac{\mu_{r21} F_2(k_2 a, B_1) - 1}{\mu_{r21} F_2(k_2 a, B_1) + 2}}{1 - f \frac{\mu_{r21} F_2(k_2 a, B_1) - 1}{\mu_{r21} F_2(k_2 a, B_1) + 2}} \tag{35}$$

Expressions for these effective medium parameters in the limit $k_1 a \ll 1$ have also been given in [35–38]. We have found that all of these papers contain at least one typographical error that must be corrected; nevertheless, when this is done we find agreement with our formulas.

The limiting cases $b = 0$, $b = a$, or $\epsilon_3 = \epsilon_2$ and $\mu_3 = \mu_2$ of (34)–(35) are all readily obtained, and can be verified to reduce to the appropriate versions of Lewin's formulas (17)–(18). Another interesting limiting

case is when k_2a (and thus also k_2b) is $\ll 1$, but k_3b remains arbitrary. If we use the approximations (A7) in (32)–(33), we obtain

$$F_2(k_2a, A_1) = \frac{\epsilon_{r32}F(k_3b)(1+2f_b)+2(1-f_b)}{\epsilon_{r32}F(k_3b)(1-f_b)+(2+f_b)} \tag{36}$$

$$F_2(k_2a, B_1) = \frac{\mu_{r32}F(k_3b)(1+2f_b)+2(1-f_b)}{\mu_{r32}F(k_3b)(1-f_b)+(2+f_b)} \tag{37}$$

where

$$f_b = \frac{b^3}{a^3} \tag{38}$$

is the fraction of the total sphere volume occupied by the inner layer (core). This result is similar to that of [38, Eqs. (14)–(15)], although the latter is based on the Bruggeman mixing formula rather than the Clausius-Mossotti formula and thus differs in detail from (36)–(37). A further case of interest is when the outer shell is electrically thin: $\delta \equiv k_2(a-b) \ll 1$, while k_2a and k_2b may be arbitrary within this constraint. In this case we use (A8) to obtain:

$$F_2(k_2a, A_1) = \frac{\epsilon_{r32}F(k_3b)+\frac{2\delta}{k_2b}}{1+\epsilon_{r32}F(k_3b)\delta\left(\frac{1}{k_2b}-\frac{k_2b}{2}\right)} \tag{39}$$

$$F_2(k_2a, B_1) = \frac{\mu_{r32}F(k_3b)+\frac{2\delta}{k_2b}}{1+\mu_{r32}F(k_3b)\delta\left(\frac{1}{k_2b}-\frac{k_2b}{2}\right)} \tag{40}$$

These limiting cases can be useful in determining approximate conditions under which the effective parameters will take on desired values — negative ones, for example.

3. NUMERICAL RESULTS

In this section we will present numerical results based on formulas (34)–(35) for the effective parameters of the layered-sphere metamaterial. We have chosen to use dielectric materials typical of what can be obtained commercially [40–44]. All permeabilities are taken to be that of free space ($\mu_1 = \mu_2 = \mu_3 = \mu_0$). The permittivity of the background medium is taken to be that of free space ($\epsilon_1 = \epsilon_0$) in all our examples, but could easily be scaled to other values if desired.

As a first example, the inner core is chosen to have a complex relative permittivity $\epsilon_{r3} = \epsilon_3/\epsilon_0 = 100\left(1 - j10^{-3}\right)$ while that of the shell is $\epsilon_{r2} = \epsilon_2/\epsilon_0 = 9.5\left(1 - j2 \times 10^{-4}\right)$. The lattice constant of the array was $p = 10\,\text{mm}$, for operation in the X-band microwave region.

A "brute force" search was carried out by varying the radii a and b of the shell and core of the layered sphere until a combination was found such that the real parts of ϵ_{eff} and μ_{eff} both became negative over the same frequency band. This was found to occur for $a = 4.66\,\text{mm}$ and $b = 2.25\,\text{mm}$, for which $\epsilon_{\text{r,eff}} = \epsilon_{\text{eff}}/\epsilon_1$ and $\mu_{\text{r,eff}} = \mu_{\text{eff}}/\mu_1$ are plotted in Fig. 3. We see that it is the second resonances in $\epsilon_{\text{r,eff}}$ and $\mu_{\text{r,eff}}$ that have been overlapped (we have not been successful in overlapping the lowest resonances using ordinary dielectric materials) at a frequency of about 11.2 GHz; above this frequency is a band of negative refractive index that ranges from 11.25 GHz to 12.4 GHz.

It could be objected at this point that the electrical length of the lattice constant is rather high at the frequencies where the

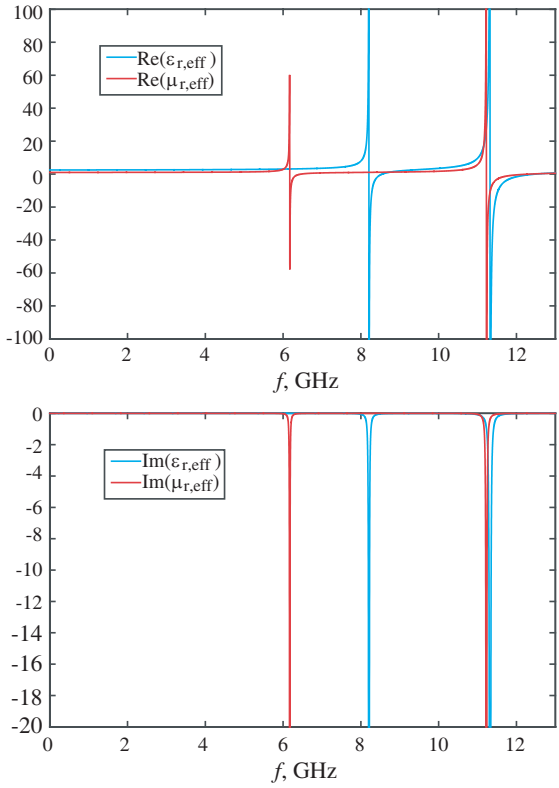

Figure 3. Real and imaginary parts of $\epsilon_{\text{r,eff}}$ and $\mu_{\text{r,eff}}$ as functions of frequency for a dielectric layered-sphere metamaterial from (34)–(35); $\epsilon_{r3} = 100\left(1 - j10^{-3}\right)$, $\epsilon_{r2} = 9.5\left(1 - j2 \times 10^{-4}\right)$, $p = 10\,\text{mm}$, $a = 4.66\,\text{mm}$ and $b = 2.25\,\text{mm}$.

negative refractive index appears: $k_0 p \simeq 2.5$ (at $k_0 p = \pi$ we might expect higher-order Bloch modes to become significant). Thus, for comparison, we have also obtained the effective parameters for this medium using two independent techniques based on numerical simulations. The first is a method described in [39] in which the reflection and transmission coefficients of a plane wave from a single layer of the dielectric spheres are computed numerically using Ansoft's HFSS (version 11.0) finite-element software. From these computations, the polarizabilities of the particles are inferred, and then the bulk effective permittivity and permeability are found from the Clausius-Mossotti formulas. The HFSS results are shown in Fig. 4. In comparing the HFSS results to those obtained from the analytical formulas (34)–(35), we see that the second resonant frequencies (and hence the band over which negative refractive index occurs) differ by less than 4% for the permittivity and less than 3% for the permeability.

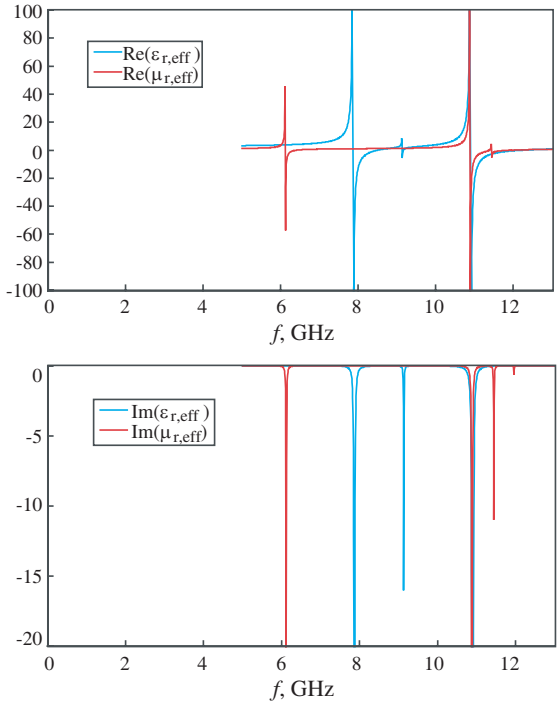

Figure 4. Real and imaginary parts of $\epsilon_{\mathrm{r,eff}}$ and $\mu_{\mathrm{r,eff}}$ as functions of frequency for a dielectric layered-sphere metamaterial from HFSS and the method of [39]; $\epsilon_{r3} = 100\left(1 - j10^{-3}\right)$, $\epsilon_{r2} = 9.5\left(1 - j2 \times 10^{-4}\right)$, $p = 10\,\mathrm{mm}$, $a = 4.66\,\mathrm{mm}$ and $b = 2.25\,\mathrm{mm}$.

These differences are likely due to two primary causes. First, as observed above the electrical size $k_0 p$ of the lattice constant in free space is not small at these frequencies; it is even larger when measured with respect to a wavelength in the effective medium. Thus the approximation that p is small compared to a wavelength is certainly strained, and lattice-related dispersion is likely to change the effective medium parameters from those predicted by (34)–(35). In support of this, we observe that the first resonant frequency in μ differs by less than 1% between the HFSS and analytical results (although that of ϵ still shows about a 4% difference). A second potential cause of the discrepancy is that the spheres are very closely packed: $2a/p = 0.932$. In this case, the neglect of interactions other than through the dipole fields in our analytic formulas is suspect, and likely to result in a certain amount of error in the model. The first source of error can be estimated by using Eqs. (20)–(24) in (9)–(10) without the approximation $k_1 a \ll 1$. When this was done, we found that the resonances in permittivity and permeability both shifted downwards, by similar orders of magnitude although not by the same amounts as in the HFSS results. An indication of the effect of neglecting higher-order multipole interactions is seen in Fig. 4 in the form of small resonances occurring near 9.1 GHz in ϵ and near 11.4 GHz in μ. There is no counterpart of these in the analytical results, and we speculate that these are due to non-dipole resonances of the layered spheres. In view of all this, it is rather remarkable that the agreement between the analytical results and those of HFSS is as good as it is. Indeed, the HFSS results still predict a region of negative refractive index from $f = 10.9$ to 11.37 GHz even though the resonance frequencies for ϵ and μ are not identical to those obtained from the analytical formulas.

A second comparison was made using results from a numerical eigenmode simulation. Attempts to do this using HFSS did not yield convergent results, apparently due to the combination of high dielectric contrast and the spherical boundaries. The simulation was therefore made using the eigensolver of CST Microwave Studio (also a finite-element program). The computed results give resonant frequencies of a period cell loaded with the layered sphere, with PEC walls at $x = 0$ and p, PMC walls at $y = 0$ and p, and a prescribed phase shift θ between the planes $z = 0$ and $z = p$. For each mode, an effective refractive index $n_{\text{eff}} = \theta/(k_0 p)$ is assigned, where k_0 is the wavenumber in free space. The dielectrics in this simulation were taken to be purely real, so that only real eigenfrequencies would be produced (the loss tangents of the materials used in the previous computations were small in any event). Only some of the modes are associated with predominantly dipolar response, and of these only some exhibit a positive slope versus

frequency; results for this subset have been plotted in Fig. 5. In the same plot, we have included the Clausius-Mossotti (CM) value of the effective refractive index

$$n_{\text{eff}} = \sqrt{\mu_{\text{r,eff}}\epsilon_{\text{r,eff}}} \qquad [\text{square root chosen so that } \text{Im}(n_{\text{eff}}) \leq 0] \quad (41)$$

in which ϵ_{eff} and μ_{eff} are obtained from (34)–(35). The limits $k_0 p n_{\text{eff}} = \pm\pi$ are also shown, to indicate the range of n_{eff} outside of which the results are likely to violate the conditions under which the effective medium model is valid. As with the HFSS results given above, qualitative agreement is good, although quantitatively the results disagree increasingly as frequency gets larger, as is to be expected. Nevertheless, a negative index of refraction is observed for the frequency range of approximately 11.2 to 12 GHz.

Making the spheres even closer to each other by choosing $p = 9.3806\,\text{mm}$ (so that $2a/p = 0.994$), we get an even wider band of frequencies for which the real part of the refractive index becomes negative, as seen in Fig. 6. However, a comparison with the results for the second resonances obtained from HFSS and displayed in Fig. 7 shows an even larger discrepancy with the analytical results than in the previous case (although the material is still DNG over a significant frequency band), which is to be expected due to the extremely close spacing of the spheres. We note that without this relatively close spacing of the spheres, we were unable to find sufficient overlap of the

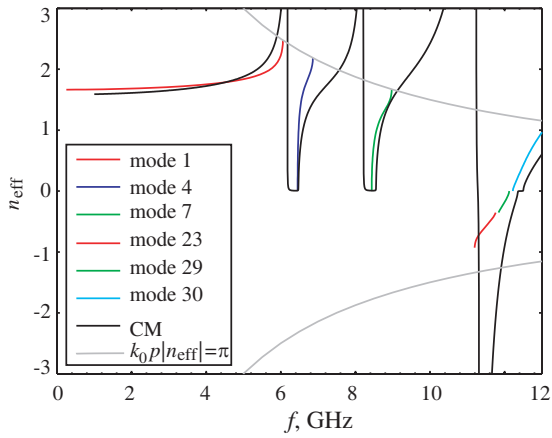

Figure 5. Real part of n_{eff} as a function of frequency for a dielectric layered-sphere metamaterial from selected eigenmodes and Clausius-Mossotti formulas (34)–(35); $\epsilon_{r3} = 100\left(1 - j10^{-3}\right)$, $\epsilon_{r2} = 9.5\left(1 - j2 \times 10^{-4}\right)$, $p = 10\,\text{mm}$, $a = 4.66\,\text{mm}$ and $b = 2.25\,\text{mm}$. Eigenmode numbers are in order of increasing resonant frequency.

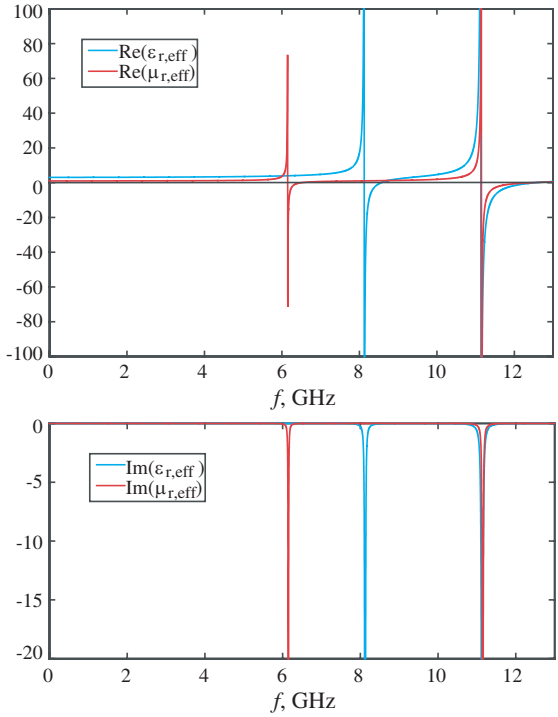

Figure 6. Real and imaginary parts of $\epsilon_{\mathrm{r,eff}}$ and $\mu_{\mathrm{r,eff}}$ as functions of frequency for a dielectric layered-sphere metamaterial from (34)–(35); $\epsilon_{r3} = 100\left(1 - j10^{-3}\right)$, $\epsilon_{r2} = 9.5\left(1 - j2 \times 10^{-4}\right)$, $p = 9.3806\,\mathrm{mm}$, $a = 4.66\,\mathrm{mm}$ and $b = 2.25\,\mathrm{mm}$.

resonances in ϵ and μ to achieve a negative refractive index. Since the results of both Fig. 6 and Fig. 7 are based on a model limited to dipole interactions between spheres, neither can be regarded as more accurate than the other, whereas the eigenmode results of Fig. 5 (that apply only to n_{eff}) can be regarded as the most accurate of the results presented in this paper.[‖]

The foregoing results show that the imaginary parts of effective ϵ_{eff} and μ_{eff} are quite large near resonances, and we must ask whether the effect of these losses is so large as to render this metamaterial impractical for applications. A fairly universal way of expressing the effect of losses is to compute the attenuation constant of a plane wave

[‖] The combination of extremely small separation distance between spheres, high dielectric contrasts and the polyhedral interpolation of the spherical surfaces frequently resulted in failure of HFSS simulations to converge. Care must be taken in choosing meshing strategies when applying any finite-element program to such configurations.

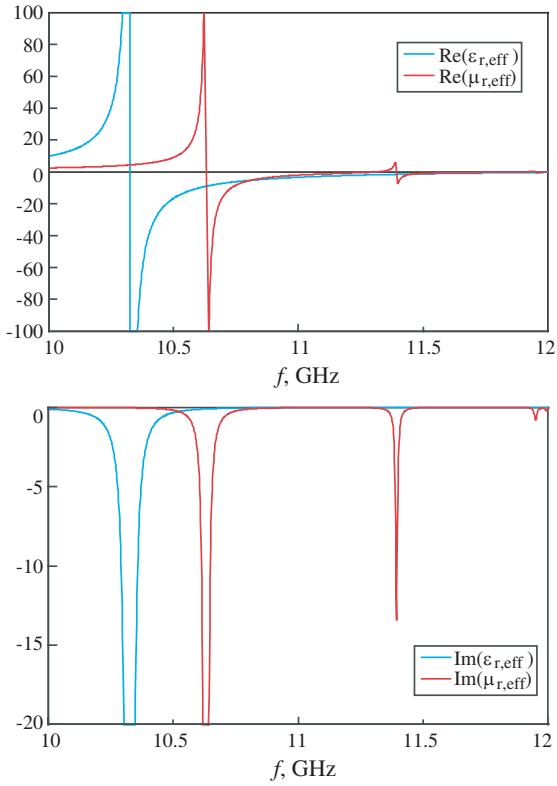

Figure 7. Real and imaginary parts of $\epsilon_{\mathrm{r,eff}}$ and $\mu_{\mathrm{r,eff}}$ as functions of frequency for a dielectric layered-sphere metamaterial from HFSS and the method of [39]; $\epsilon_{r3} = 100\left(1 - j10^{-3}\right)$, $\epsilon_{r2} = 9.5\left(1 - j2 \times 10^{-4}\right)$, $p = 9.3806\,\mathrm{mm}$, $a = 4.66\,\mathrm{mm}$ and $b = 2.25\,\mathrm{mm}$.

in dB per wavelength, i.e.,

$$\alpha_{\mathrm{dB}/\lambda} = 8.686\,(\alpha\lambda)_{\mathrm{dB}} = 54.575\frac{|\mathrm{Im}(n_{\mathrm{eff}})|}{|\mathrm{Re}(n_{\mathrm{eff}})|} = \frac{54.575}{\mathrm{FOM}} \tag{42}$$

and what has been called the figure of merit (FOM) or quality factor by some authors is defined as

$$\mathrm{FOM} = \frac{|\mathrm{Re}(n_{\mathrm{eff}})|}{|\mathrm{Im}(n_{\mathrm{eff}})|} \tag{43}$$

In Fig. 8 is shown a plot of the attenuation constant calculated from (34), (35) and (42) for the metamaterial of Fig. 6. Fig. 9 shows the corresponding values found from the HFSS simulations. In spite of the very large values this quantity takes near the resonance and near zeroes

of the real part of the refractive index, we see that the attenuation reaches a minimum of about $0.5\,\mathrm{dB}/\lambda$ at about $f = 11.8\,\mathrm{GHz}$. It is, moreover, less that $1\,\mathrm{dB}/\lambda$ over a bandwidth of about 1 GHz (nearly 10%). Similar results are obtained from the HFSS simulation, but over a smaller bandwidth (about 0.5 GHz). This is significantly better than results for other types of negative-index metamaterials that have been reported in the literature, as we now show.

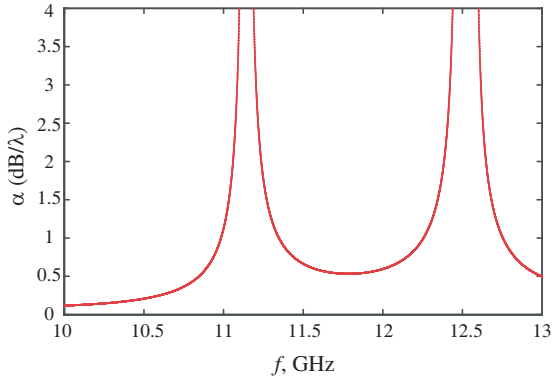

Figure 8. Attenuation constant in dB/λ from analytical formula as a function of frequency for a dielectric layered-sphere metamaterial with $\epsilon_{r3} = 100\left(1 - j10^{-3}\right)$, $\epsilon_{r2} = 9.5\left(1 - j2 \times 10^{-4}\right)$, $p = 9.3806\,\mathrm{mm}$, $a = 4.66\,\mathrm{mm}$ and $b = 2.25\,\mathrm{mm}$.

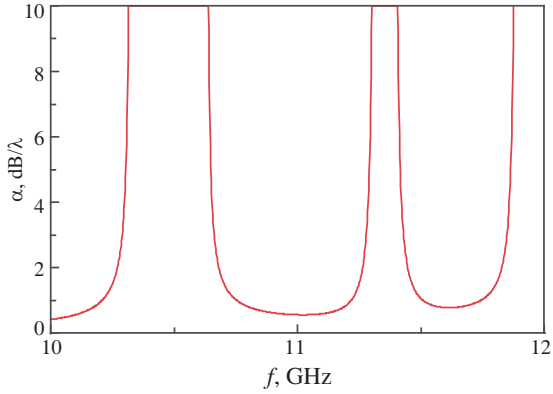

Figure 9. Attenuation constant in dB/λ from HFSS computations as a function of frequency for a dielectric layered-sphere metamaterial with $\epsilon_{r3} = 100\left(1 - j10^{-3}\right)$, $\epsilon_{r2} = 9.5\left(1 - j2 \times 10^{-4}\right)$, $p = 9.3806\,\mathrm{mm}$, $a = 4.66\,\mathrm{mm}$ and $b = 2.25\,\mathrm{mm}$.

Table 1. Comparison of figures of merit (FOM) and bulk attenuation of some negative-index metamaterials.

Metamaterial	Freq.	FOM	$\alpha_{\mathrm{dB}/\lambda}$
[45] Modified split-ring/rod structure	4.5 GHz	0.7	75
[16] Layered spheres (Drude/$LiTaO_3$)	3.65 THz	0.6	90
[46] Layered Au film (elliptical holes)	167 THz	2	27
[47] Perforated metal-dielectric stacks	176 THz	25	2.18
[48] Layered Ag film (rect. holes)	212 THz	3	18
[49] Conventional split-rings/rods	100 GHz	5	11
[50] Metal rod/ferrite composite	22 GHz	10.9	5
[51] Metal rod/ferrite composite	10 GHz	6.8	8
[52] Perforated "double-fishnet"	214 THz	3	18
[7] Binary spheres (Drude/$LiTaO_3$)	3.85 THz	0.5	105
[17] Layered spheres (Au/CuCl)	775 THz	0.2	247
[53] Layered metal film ("fishnet")	250 THz	3.6	15
[18] Layered spheres in liquid crystal	107 THz	0.8	67
[54] Bilayer printed metalization	14 GHz	5.5	10
[55] Optimized layered metal film	275 THz	3.9	14
[56] Meander-line/loaded loops	400 MHz	0.7	75
[57] Layered metallic cross-pairs	1 THz	10.9	5
[58] Multilayered "fishnet"	169 THz	3.5[¶]	16
[59] "Fishnet" structure	517 THz	0.3	182
[60] Cut wire pairs (birefringent)	1.3 THz	23	2.4
[61] Cylindrical dielectric resonators	10 GHz	14	3.9
[62] Split cubes in a cage	176 THz	0.3	165
[63] "Fishnet" structure	1 THz	5	10.9
[64] Cut wire pair array	155 THz	2.1	25
[65] Split-ring resonator array	100 GHz	12.5	4.4
[66] Coaxial channel array	600 THz	11.4	4.8
[67] Silver ring array	515 THz	11	5
[68] Rodded silver sphere array	606 THz	2.5	22
[69] "Fishnet" structure	400 THz	3.34[+]	16.3

[¶] Measured value; simulated value was 18.
[+] Measured value

Not all publications about specific passive negative-index metamaterials provide data on both real and imaginary parts of the refractive index; often the calculated or measured results provide only values of the power transmission coefficient for a layer of the metamaterial. We have identified a number of papers, however, that do present sufficient data to obtain values of FOM and $\alpha_{\mathrm{dB}/\lambda}$ with which our results can be compared, although we do not make any claim of completeness for this list. When FOM or $\alpha_{\mathrm{dB}/\lambda}$ was not given in these papers, attenuation data has been extracted from the plots therein (this could not always be done with high accuracy) and converted. The results are assembled and displayed in Table 1.

We see that many of the materials listed are very lossy, and that, in principle, the all-dielectric layered-sphere metamaterial proposed here is capable of providing an order-of-magnitude reduction over all but a few of the best attenuations per wavelength currently achieved for a negative-index metamaterial. It should, of course, be kept in mind that other factors such as frequency, bandwidth and value of the real part of the negative refractive index are also significant in assessing the quality of a negative-index metamaterial. For example, it is generally more difficult to attain low attenuation at infrared and optical frequencies than at microwave or millimeter-wave frequencies.

An alternative nonmagnetic structure was found that also provides negative-index behavior: an array of dielectric-coated metal spheres. In this structure, the core region of the layered sphere in Fig. 2 is made of a good conductor, such as copper. It is modeled by giving the core region a complex permittivity $\epsilon_3 = \epsilon_3' - j\sigma/\omega$, where ϵ_3' is the real part of the permittivity of the metal (usually ϵ_0 if the metal is nonmagnetic) and σ is the conductivity of the metal. The large imaginary part of the complex core permittivity has the effect of suppressing many of the resonances of the layered sphere, leaving only ones whose fields are concentrated in the outer dielectric layer. We chose the shell permittivity to be $\epsilon_{r2} = 100\left(1 - j10^{-3}\right)$, while the core was copper ($\sigma = 5.7 \times 10^7\,\mathrm{S/m}$). The lattice constant of the array was chosen to be $p = 12.481\,\mathrm{mm}$, and a much lower frequency range (2 to 4 GHz) was explored. Again, we experimented with various combinations of inner and outer radii, and arrived at a sphere for which $a = 6.2\,\mathrm{mm}$ and $b = 2.9\,\mathrm{mm}$. The values of $\epsilon_{\mathrm{r,eff}}$ and $\mu_{\mathrm{r,eff}}$ are plotted in Fig. 10.

We see that in this case, the resonance in permittivity is narrower than in the case of the all-dielectric layered spheres. This results in a smaller fractional bandwidth of negative-index operation: 2.81 to 2.87 GHz (note that at these frequencies the lattice constant in this example is much smaller compared to a free space wavelength than in the previous example: $k_0 p = 0.745$). Additionally, when we examine

the attenuation per wavelength (shown in Fig. 11), we see that its minimum value in the negative-index region is substantially larger than that predicted for the all-dielectric layered-sphere metamaterial already considered: 3.2 dB/λ at 2.85 GHz. However, this is still significantly lower than the values reported above for other negative-index media in Table 1, although it is attained over a much narrower bandwidth (about 0.1 GHz) than in the all-dielectric case. It is likely that this loss is lower than that of other metal-based metamaterials because of the simpler and smoother shape of the metal used, resulting in a lower contribution of ohmic losses to the total attenuation. Final confirmation of these predictions must, of course, come from experimental measurements.

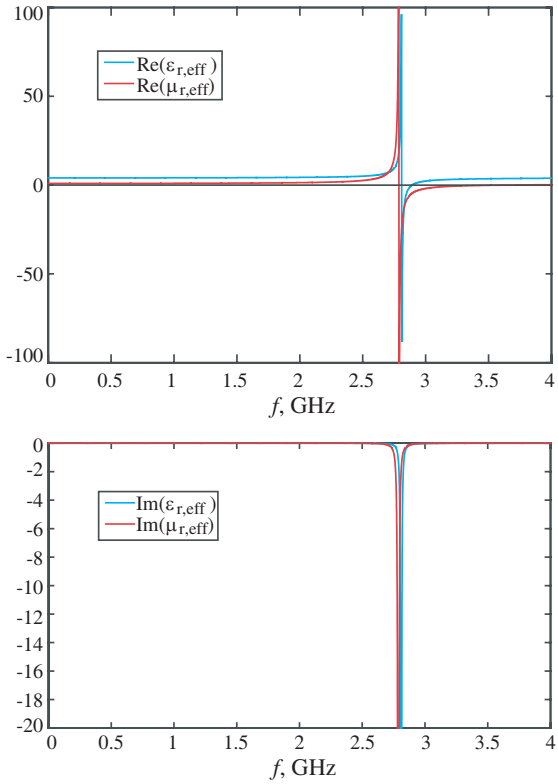

Figure 10. Real and imaginary parts of $\epsilon_{\mathrm{r,eff}}$ and $\mu_{\mathrm{r,eff}}$ as functions of frequency for a dielectric-coated copper-sphere metamaterial from (34)–(35); $\sigma = 5.7 \times 10^7$ S/m, $\epsilon_{r2} = 100\left(1 - j10^{-3}\right)$, $p = 12.481$ mm, $a = 6.2$ mm and $b = 2.9$ mm.

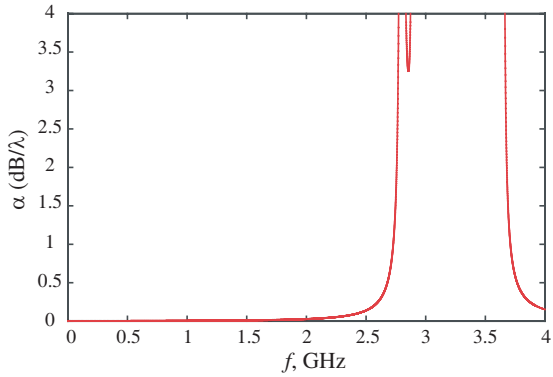

Figure 11. Attenuation constant in dB/λ as a function of frequency for a dielectric-coated copper-sphere metamaterial from (34)–(35); $\sigma = 5.7 \times 10^7\,\mathrm{S/m}$, $\epsilon_{r2} = 100\left(1 - j10^{-3}\right)$, $p = 12.481\,\mathrm{mm}$, $a = 6.2\,\mathrm{mm}$ and $b = 2.9\,\mathrm{mm}$.

Both of our proposed metamaterials resemble to some extent the one proposed in [16], in that both are arrays of layered spheres. However, in [16], where the intended frequency range is several THz, the resonance of each sphere is achieved by having the outer layer be a Drude medium (a metal or semiconductor) with negative permittivity and a loss tangent on the order of 10^{-2} in the terahertz region, while the inner core is $LiTaO_3$, a high-permittivity dielectric with a similar value of loss tangent. The losses inherent in these materials result in an attenuation of over $90\,\mathrm{dB}/\lambda$ at a frequency of 3.65 THz, where the lowest losses in the negative-index range were attained.

4. CONCLUSION

In this paper we have proposed a novel passive metamaterial that exhibits negative refractive index and much lower loss at microwave frequencies than typical split-ring/rod-based media. Bandwidths of greater than 10% for negative-index behavior are predicted, and implementation using commercially available materials should be possible at microwave frequencies. Results from analytical formulas are validated by comparisons with two independent numerical simulations.

In future investigations, we plan to fabricate prototypes of these proposed metamaterials, and carry out measurements to confirm both the predicted negative-index behavior and the low attenuation. Of course, fabrication of metamaterials based on spherical particles is likely to be challenging by comparison with those based on a printed-

circuit structure. In principle, there is nothing essential about using spherically shaped particles; other shapes such as cubes could equally serve the desired purpose. The advantage of the spherical geometry is that closed-form expressions are available for the polarizabilities of the particles, making design much less computationally intensive. Metamaterials based on arrays of nonspherical dielectric scatterers will be the subject of a future publication. Also of interest would be to extend the analysis to spheres with more than two layers, and to implement a more systematic method of searching for negative-index configurations. Finally, the extension of the ideas of this paper to millimeter-wave, terahertz and higher frequencies would be worth examining. Such extensions will depend on the availability of suitable low-loss dielectrics and metals at these frequencies, which also will merit further research.

ACKNOWLEDGMENT

This work was supported by the US National Science Foundation grant ECS-0524710. Further support was furnished by Sandia National Laboratories.

APPENDIX A. SOME PROPERTIES OF THE FUNCTIONS C_1–C_3

From the definitions (29)–(31) of the functions C_1–C_3, we see that

$$C_2(z_1,z_2)=\frac{\partial C_1(z_1,z_2)}{\partial z_2};\quad C_3(z_1,z_2)=\frac{\partial C_2(z_1,z_2)}{\partial z_1}=\frac{\partial^2 C_1(z_1,z_2)}{\partial z_1\partial z_2} \tag{A1}$$

In [70] is proved the following expression, which allows C_3 to be expressed in terms of C_1 and C_2:

$$C_1(z_1,z_2)C_3(z_1,z_2)+C_2(z_1,z_2)C_2(z_2,z_1)=1 \tag{A2}$$

By inserting expressions (7) and (8) for the Riccati-Bessel functions into (29)–(31) and using some trigonometric identities, we find that only trigonometric functions of the difference z_1-z_2 need appear in the formulas for C_1–C_3:

$$C_1(z_1,z_2)=\left(1+\frac{1}{z_1z_2}\right)\sin(z_1-z_2)+\left(\frac{1}{z_1}-\frac{1}{z_2}\right)\cos(z_1-z_2) \tag{A3}$$

$$C_2(z_1,z_2)=\left(\frac{1}{z_1}-\frac{1}{z_2}-\frac{1}{z_1z_2^2}\right)\sin(z_1-z_2)+\left(\frac{1}{z_2^2}-\frac{1}{z_1z_2}-1\right)\cos(z_1-z_2) \tag{A4}$$

$$C_3(z_1,z_2)=\left(\frac{1}{z_1^2z_2^2}-\frac{1}{z_1^2}-\frac{1}{z_2^2}+\frac{1}{z_1z_2}+1\right)\sin(z_1-z_2)$$
$$+(z_2-z_1)\left(\frac{1}{z_1z_2}+\frac{1}{z_1^2z_2^2}\right)\cos(z_1-z_2) \tag{A5}$$

from which in particular we have

$$C_1(z_1,z_1)=C_3(z_1,z_1)=0; \qquad C_2(z_1,z_1)=-1 \tag{A6}$$

If $z_1\to 0$ while z_2/z_1 remains constant, we have

$$C_1(z_1,z_2)\simeq\frac{z_1^3-z_2^3}{3z_1z_2}; \qquad C_2(z_1,z_2)\simeq-\frac{z_1^3+2z_2^3}{3z_1z_2^2};$$
$$C_3(z_1,z_2)\simeq-\frac{2}{3}\frac{z_1^3-z_2^3}{z_1^2z_2^2} \tag{A7}$$

Finally, if $|z_1-z_2|\ll 1$ while z_1 and z_2 themselves may be of arbitrary magnitude, we have, with errors of $\mathcal{O}[(z_1-z_2)^2]$:

$$C_1(z_1,z_2)\simeq z_1-z_2; \qquad C_2(z_1,z_2)\simeq -1;$$
$$C_3(z_1,z_2)\simeq(z_1-z_2)\left(1-\frac{2}{z_2^2}\right) \tag{A8}$$

REFERENCES

1. Smith, D. R., W. J. Padilla, D. C. Vier, S. C. Nemat-Nasser, and S. Schultz, "Composite medium with simultaneously negative permeability and permittivity," *Phys. Rev. Lett.*, Vol. 84, 4184–4187, 2000.
2. Holloway, C. L., E. F. Kuester, J. Baker-Jarvis, and P. Kabos, "A double negative (DNG) composite medium composed of magneto-dielectric spherical particles embedded in a matrix," *IEEE Trans. Ant. Prop.*, Vol. 51, 2596–2603, 2003.
3. Vendik, O. G. and M. S. Gashinova, "Artificial double negative (DNG) media composed by two different dielectric sphere lattices embedded in a dielectric matrix," *Proceedings 34th European Microwave Conference*, 1209–1212, Amsterdam, October 12–14, 2004.
4. Vendik, I. B., O. G. Vendik, and M. S. Gashinova, "Artificial dielectric medium possessing simultaneously negative permittivity and magnetic permeability," *Pisma Zhurn. Tekh. Fiz.*, Vol. 32, No. 10, 30–39, 2006 (in Russian); *Tech. Phys. Lett.*, Vol. 32, 429–432, 2006 (in English).

5. Jylhä, L., I. Kolmakov, S. Maslovski, and S. Tretyakov, "Modeling of isotropic backward-wave materials composed of resonant spheres," *J. Appl. Phys.*, Vol. 99, art. 043102, 2006.
6. Vendik, I., O. Vendik, I. Kolmakov, and M. Odit, "Modelling of isotropic double negative media for microwave applications," *Opto-Electron. Rev.*, Vol. 14, 179–186, 2006.
7. Yannopapas, V., "Negative refraction in random photonic alloys of polaritonic and plasmonic microspheres," *Phys. Rev. B*, Vol. 75, art. 035112, 2007.
8. Ahmadi, A. and H. Mosallaei, "Physical configuration and performance modeling of all-dielectric metamaterials," *Phys. Rev. B*, Vol. 77, art. 045104, 2008.
9. Vendik, I. B., M. A. Odit, and D. S. Kozlov, "3D isotropic metamaterial based on a regular array of resonant dielectric spherical inclusions," *Metamaterials*, Vol. 3, 140–147, 2009.
10. Ghadarghadr, S. and H. Mosallaei, "Dispersion diagram characteristics of periodic array of dielectric and magnetic materials based spheres," *IEEE Trans. Ant. Prop.*, Vol. 57, 149–160, 2009.
11. Vendik, I., M. Odit, and D. Kozlov, "3D metamaterial based on a regular array of resonant dielectric inclusions," *Radioengineering*, Vol. 18, 111–116, 2009.
12. Shore, R. and A. D. Yaghjian, "Traveling waves on three-dimensional periodic arrays of two different alternating magnetodielectric spheres," *IEEE Trans. Ant. Prop.*, Vol. 57, 3077–3091, 2009.
13. Vendik, I. B., O. G. Vendik, and M. A. Odit, "An isotropic metamaterial formed with ferroelectric ceramic spherical inclusions," *Fiz. Tverd. Tela*, Vol. 51, 1499–1503, 2009 (in Russian); *Phys. Solid State*, Vol. 51, 1590–1594, 2009 (in English).
14. Yannopapas, V. and A. Moroz, "Negative refractive index metamaterials from inherently non-magnetic materials for deep infrared to terahertz frequency ranges," *J. Phys. Cond. Mat.*, Vol. 17, 3717–3734, 2005.
15. Seo, B.-J., T. Ueda, T. Itoh, and H. Fetterman, "Isotropic left handed material at optical frequency with dielectric spheres embedded in negative permittivity medium," *Appl. Phys. Lett.*, Vol. 88, art. 161122, 2006.
16. Wheeler, M. S., J. S. Aitchison, and M. Mojahedi, "Coated nonmagnetic spheres with a negative index of refraction at infrared frequencies," *Phys. Rev. B*, Vol. 73, art. 045105, 2006.

17. Yannopapas, V., "Negative refractive index in the near-UV from Au-coated CuCl nanoparticle superlattices," *Phys. Stat. Sol. (RRL)*, Vol. 1, 208–210, 2007.
18. Khoo, I. C., A. Diaz, D.-H. Kwon, and D. H. Werner, "Liquid crystalline nonlinear optical metamaterials with low-loss tunable negative-zero-positive refractive indices," *Proc. SPIE*, Vol. 6587, art. 658702, 2007.
19. Alù, A. and N. Engheta, "Polarizabilities and effective parameters for collections of spherical nanoparticles formed by pairs of concentric double-negative, single-negative, and/or double-positive metamaterial layers," *J. Appl. Phys.*, Vol. 97, art. 094310, 2005.
20. Mie, G., "Beiträge sur Optik trüber Medien, speziell kolloidaler Metallösungen," *Ann. Physik*, 4th Folge, Bd. 25, 377–445, 1908; *Library Translation 1873*, Royal Aircraft Establishment, London, UK, 1976 (in English); *Report SAND78-6018*, Sandia Laboratories, Albuquerque, NM, 1978.
21. Kerker, M., *Scattering of Light and Other Electromagnetic Radiation*, Academic Press, New York, 1969.
22. Keller, O., "Optical works of L. V. Lorenz," *Progress in Optics*, E. Wolf, ed., Vol. 43, 195–294, Elsevier, Amsterdam, 2002.
23. Gans, R. and H. Happel, "Zur Optik kolloidaler Metallösungen," *Ann. Physik*, 4th Folge, Bd. 29, 277–300, 1909.
24. Stratton, J. A., "The effect of rain and fog on the propagation of very short radio waves," *Proc. IRE*, Vol. 18, 1064–1074, 1930.
25. Kreibig, U. and M. Vollmer, *Optical Properties of Metal Clusters*, 144, Springer-Verlag, Berlin, 1995.
26. Bohren, C. F. and D. R. Huffman, *Absorption and Scattering of Light by Small Particles*, Wiley, New York, 1983.
27. Abramowitz, M. and I. A. Stegun, *Handbook of Mathematical Functions*, Chapter 10, U. S. Government Printing Office, Washington DC, 1964.
28. Lewin, L., "The electrical constants of a material loaded with spherical particles," *J. IEE (London)*, Part III, Vol. 94, 65–68, 1947.
29. Khizhnyak, N. A., "Artificial anisotropic dielectrics: I, II and III," *Zh. Tekh. Fiz.*, Vol. 27, 2006–2013, 2014–2026 and 2027–2037, 1957 (in Russian); *Sov. Phys. Tech. Phys.*, Vol. 2, 1858–1864, 1865–1876 and 1877–1886, 1957 (in English).
30. Aden, A. L. and M. Kerker, "Scattering of electromagnetic waves from two concentric spheres," *J. Appl. Phys.*, Vol. 22, 1242–1246,

1951.

31. Güttler, A., "Die Miesche Theorie der Beugung durch dielektrische Kugeln mit absorbierendem Kern und ihre Bedeutung für Probleme der interstellaren Materie und des atmosphärischen Aerosols," *Ann. Physik*, 6th Folge, Bd. 11, 65–98, 1952.
32. Shifrin, K. S., "Scattering of light from two-layer particles," *Izv. Akad. Nauk SSSR Ser. Geofiz.*, No. 2, 15–21, 1952 (in Russian).
33. Fenn, R. W. and H. Oser, "Scattering properties of concentric soot-water spheres for visible and infrared light," *Appl. Opt.*, Vol. 4, 1504–1509, 1965.
34. Krekov, G. M. and R. F. Rakhimov, "Calculation of radiation characteristics of polydisperse concentric spheres," *Izv. VUZ Fiz.*, No. 6, 30–35, 1973 (in Russian); *Sov. Phys. J.*, Vol. 16, 762–766, 1973 (in English).
35. Galst'yan, E. A. and A. A. Ravaev, "Electrodynamic parameters of a medium containing two-layer spherical inclusions," *Izv. VUZ Radiofiz.*, Vol. 30, 1243–1248, 1987 (in Russian); *Radiophys. Quant. Electron.*, Vol. 30, 918–922, 1987 (in English).
36. Ponomarenko, V. I., V. N. Berzhanskii, S. I. Zhuravlev and E. D. Pershina, "Permittivity and permeability of a synthetic dielectric with metal-plated ferrite particles at microwave frequencies," *Radiotekh. Elektron.*, Vol. 35, 2208–2211, 1990 (in Russian); *Sov. J. Commun. Technol. Electron.*, Vol. 36, No. 3, 133–136, 1991 (in English).
37. Ponomarenko, V. I. and D. I. Mirovitskii, "An artificial dielectric with metallized magnetodielectric inserts," *Radiotekhnika*, Vol. 46, No. 6, 76–78, 1991 (in Russian); *Telecommun. Radio Eng.*, Vol. 46, No. 5, 104–107, 1991 (in English).
38. Timoshenko, A. M. and V. I. Ponomarenko, "A generalized formula for the electromagnetic constants of a medium with spherical inclusions," *Radiotekh. Elektron.*, Vol. 41, 412–415, 1996 (in Russian); *J. Commun. Technol. Electron.*, Vol. 41, 379–382, 1996 (in English).
39. Scher, A. D. and E. F. Kuester, "Extracting the bulk effective parameters of a metamaterial via the scattering from a single planar array of particles," *Metamaterials*, Vol. 3, 44–55, 2009.
40. Trans-Tech Incorporated, http://www.trans-techinc.com.
41. Morgan Electro Ceramics Ltd., http://www.morganelectroceramics.com.
42. TCI Ceramics, http://www.magneticsgroup.com.
43. Temex Ceramics, http://www.temex-ceramics.com.

44. Pacific Ceramics, http://www.pceramics.com.
45. Schussler, M., A. Fleckenstein, J. Freese, and R. Jakoby, "Left-handed metamaterials based on split ring resonators for microstrip applications," *33rd European Microwave Conference*, 1119–1122, 2003.
46. Zhang, S., W. Fan, K. J. Malloy, S. R. J. Brueck, N. C. Panoiu, and R. M. Osgood, "Demonstration of metal-dielectric negative-index metamaterials with improved performance at optical frequencies," *J. Opt. Soc. Amer. B*, Vol. 23, 434–438, 2006.
47. Zhang, S., W. Fan, N. C. Panoiu, K. J. Malloy, R. M. Osgood, and S. R. J. Brueck, "Optical negative-index bulk metamaterials consisting of 2D perforated metal-dielectric stacks," *Opt. Express*, Vol. 14, 6778–6787, 2006.
48. Dolling, G., C. Enkrich, M. Wegener, C. M. Soukoulis, and S. Linden, "Low-loss negative-index metamaterial at telecommunication wavelengths," *Opt. Lett.*, Vol. 31, 1800–1802, 2006.
49. Gokkavas, M., K. Guven, I. Bulu, K. Aydin, R. S. Penciu, M. Kafesaki, C. M. Soukoulis, and E. Ozbay, "Experimental demonstration of a left-handed metamaterial operating at 100 GHz," *Phys. Rev. B*, Vol. 73, art. 193103, 2006.
50. He, Y., P. He, V. G. Harris, and C. Vittoria, "Role of ferrites in negative index metamaterials," *IEEE Trans. Magnetics*, Vol. 42, 2852–2854, 2006.
51. He, Y., P. He, S. D. Yoon, P. V. Parimi, F. J. Rachford, V. G. Harris, and C. Vittoria, "Tunable negative index metamaterial using yttrium iron garnet," *J. Mag. Mag. Mater.*, Vol. 313, 187–191, 2007.
52. Dolling, G., M. Wegener, C. M. Soukoulis, and S. Linden, "Design-related losses of double-fishnet negative-index photonic metamaterials," *Opt. Express*, Vol. 15, 11536–11541, 2007.
53. Koschny, T., J. Zhoua, and C. M. Soukoulis, "Magnetic response and negative refractive index of metamaterials," *Proc. SPIE*, Vol. 6581, art. 658103, 2007.
54. Guven, K., A. O. Cakmak, M. D. Caliskan, T. F. Gundogdu, M. Kafesaki, C. M. Soukoulis, and E Ozbay, "Bilayer metamaterial: Analysis of left-handed transmission and retrieval of effective medium parameters," *J. Opt. A*, Vol. 9, S361–S365, 2007.
55. Kildishev, A. V., U. K. Chettiar, V. M. Shalaev, D.-H. Kwon, Z. Bayraktar, and D. H. Werner, "Stochastic optimization of low-

loss optical negative-index metamaterial," *J. Opt. Soc. Amer. B*, Vol. 24, A34–A39, 2007.

56. Erentok, A., R. W. Ziolkowski, J. A. Nielsen, R. B. Greegor, C. G. Parazzoli, M. H. Tanielian, S. A. Cummer, B.-I. Popa, T. Hand, D. C. Vier, and S. Schultz, "Low frequency lumped element-based negative index metamaterial," *Appl. Phys. Lett.*, Vol. 91, art. 184104, 2007.
57. Paul, O., C. Imhof, B. Reinhard, R. Zengerle, and R. Beigang, "Negative index bulk metamaterial at terahertz frequencies," *Opt. Express*, Vol. 16, 6736–6744, 2008.
58. Valentine, J., S. Zhang, T. Zentgraf, E. Ulin-Avila, D. A. Genov, G. Bartal, and X. Zhang, "Three-dimensional optical metamaterial with a negative refractive index," *Nature*, Vol. 455, 376–379, 2008.
59. Xiao, S., U. K. Chettiar, A. V. Kildishev, V. P. Drachev, and V. M. Shalaev, "Yellow-light negative-index metamaterials," *Opt. Lett.*, Vol. 34, 3478–3480, 2009.
60. Weis, P., O. Paul, C. Imhof, R. Beigang, and M. Rahm, "Strongly birefringent metamaterials as negative index terahertz wave plates," *Appl. Phys. Lett.*, Vol. 95, art. 171104, 2009.
61. Lepetit, T., E. Akmansoya, and J.-P. Ganneb, "All-dielectric metamaterial: A ferroelectric-based scheme in the microwave range," *Proc. SPIE*, Vol. 7392, art. 73920H, 2009.
62. Andryieuski, A., C. Menzel, C. Rockstuhl, R. Malureanu, and A. V. Lavrinenko, "The split cube in a cage: Bulk negative-index material for infrared applications," *J. Opt. A*, Vol. 11, art. 114010, 2009.
63. Ding, P., E. J. Liang, W. Q. Hu, L. Zhang, Q. Zhou, and Q. Z. Xue, "Numerical simulations of terahertz double-negative metamaterial with isotropic-like fishnet structure," *Photon. Nanostruct. Fund. Appl.*, Vol. 7, 92–100, 2009.
64. Kanté, B., A. de Lustrac, and J.-M. Loutioz, "Low loss negative index metamaterials with one type of meta-atom," *Photon. Nanostruct. Fund. Appl.*, Vol. 8, 112–119, 2010.
65. Alici, K. B. and E. Ozbay, "Theoretical study and experimental realization of a low-loss metamaterial operating at the millimeter-wave regime: Demonstrations of flat- and prism-shaped samples," *IEEE J. Selected Topics Quant. Electron.*, Vol. 16, 386–393, 2010.
66. Burgos, S. P., R. de Waele, A. Polman, and H. A. Atwater, "A single-layer wide-angle negative-index metamaterial at visible frequencies," *Nature Materials*, Vol. 9, 407–412, 2010.

67. Tang, J. and S. He, "A novel structure for double negative NIMs towards UV spectrum with high FOM," *Opt. Express*, Vol. 18, 25256–25263, 2010.
68. Gong, B. and X. Zhao, "Numerical demonstration of a three-dimensional negative-index metamaterial at optical frequencies," *Opt. Express*, Vol. 19, 289–296, 2011.
69. García-Meca, C., J. Hurtado, J. Martí, A. Martínez, W. Dickson, and A. V. Zayats, "Low-loss multilayered metamaterial exhibiting a negative index of refraction at visible wavelengths," *Phys. Rev. Lett.*, Vol. 106, art. 067402, 2011.
70. Goodwin, E. T., "Recurrence relations for cross products of Bessel functions," *Quart. J. Mech. Appl. Math.*, Vol. 2, 72–74, 1949.